Generation and transmission of 85.4 Gb/s real-time 16QAM coherent optical OFDM signals over 400 km SSMF with preamble-less reception

Rachid Bouziane,[1,*] Rene Schmogrow,[2] D. Hillerkuss,[2] P. A. Milder,[3] C. Koos,[2] W. Freude,[2] J. Leuthold,[2] P. Bayvel,[1] and R. I. Killey[1]

[1] *Optical Networks Group, Department of Electronic and Electrical Engineering, (UCL) University College London, Torrington Place, London, WC1E 7JE, UK*

[2] *Institute of Photonics and Quantum Electronics (IPQ), Karlsruhe Institute of Technology (KIT), 76131 Karlsruhe, Germany*

[3] *Department of Electrical and Computer Engineering, Carnegie Mellon University, 5000 Forbes Ave., Pittsburgh, PA 15213, USA*

[*] *r.bouziane@ee.ucl.ac.uk*

Abstract: This paper presents a real-time, coherent optical OFDM transmitter based on a field programmable gate array implementation. The transmitter uses 16QAM mapping and runs at 28 GSa/s achieving a data rate of 85.4 Gb/s on a single polarization. A cyclic prefix of 25% of the symbol duration is added enabling dispersion-tolerant transmission over up to 400 km of SSMF. This is the first transmission experiment performed with a real-time OFDM transmitter running at data rates higher than 40 Gb/s. A key aspect of the paper is the introduction of a novel method for OFDM symbol synchronization without relying on training symbols. Unlike conventional preamble-based synchronization methods which perform cross-correlations at regular time intervals and let the system run freely in between, the proposed method performs synchronization in a continuous manner ensuring correct symbol alignment at all times.

OCIS codes: (060.4080) Modulation; (060.4510) Optical communications.

References and links

1. W. Shieh, H. Bao, and Y. Tang, "Coherent optical OFDM: theory and design," Opt. Express **16**(2), 841–859 (2008).
2. N. Cvijetic, "OFDM for next generation optical access networks," J. Lightwave Technol. **30**(4), 384–398 (2012).
3. X. Q. Jin, E. Hugues-Salas, R. P. Giddings, J. L. Wei, J. Groenewald, and J. M. Tang, "First real-time experimental demonstrations of 11.25Gb/s Optical OFDMA PONs with adaptive dynamic bandwidth allocation," Opt. Express **19**(21), 20557–20570 (2011).
4. Y. Benlachtar, R. Bouziane, R. I. Killey, C. R. Berger, P. Milder, R. Koutsoyannis, J. C. Hoe, M. Püschel, and M. Glick, "Optical OFDM for the data center," in Proc. of International Conference on Transparent Optical Networks (ICTON) (2010).
5. Y. Benlachtar, P. M. Watts, R. Bouziane, P. Milder, D. Rangaraj, A. Cartolano, R. Koutsoyannis, J. C. Hoe, M. Püschel, M. Glick, and R. I. Killey, "Generation of optical OFDM signals using 21.4 GS/s real time digital signal processing," Opt. Express **17**(20), 17658–17668 (2009).
6. R. Schmogrow, M. Winter, D. Hillerkuss, B. Nebendahl, S. Ben-Ezra, J. Meyer, M. Dreschmann, M. Huebner, J. Becker, C. Koos, W. Freude, and J. Leuthold, "Real-time OFDM transmitter beyond 100 Gbit/s," Opt. Express **19**(13), 12740–12749 (2011).
7. B. Inan, S. Adhikari, O. Karakaya, P. Kainzmaier, M. Mocker, H. von Kirchbauer, N. Hanik, and S. L. Jansen, "Real-time 93.8-Gb/s polarization-multiplexed OFDM transmitter with 1024-point IFFT," Opt. Express **19**(26), B64–B68 (2011).
8. N. Kaneda, Q. Yang, X. Liu, S. Chandrasekhar, W. Shieh, and Y. Chen, "Real-time 2.5 GS/s coherent optical receiver for 53.3-Gb/s Sub-Banded OFDM," J. Lightwave Technol. **28**(4), 494–501 (2010).
9. R. Schmogrow, R. Bouziane, D. Hillerkuss, P. A. Milder, R. Koutsoyannis, R. Killey, Y. Benlachtar, P. Watts, P. Bayvel, C. Koos, W. Freude, and J. Leuthold, "85.4 Gbit/s Real-Time OFDM Signal Generation with Transmission over 400 km and Preamble-less Reception," in Proc. of Conference on Lasers and Electro-Optics (CLEO) (2012).

#173248 - $15.00 USD Received 24 Jul 2012; revised 27 Aug 2012; accepted 30 Aug 2012; published 5 Sep 2012

10. Y. Benlachtar, P. M. Watts, R. Bouziane, P. Milder, R. Koutsoyannis, J. C. Hoe, M. Püschel, M. Glick, and R. I. Killey, "Real-time digital signal processing for the generation of optical orthogonal frequency-division-multiplexed signals," IEEE J. Sel. Top. Quantum Electron. **16**(5), 1235–1244 (2010).
11. P. A. Milder, F. Franchetti, J. C. Hoe, and M. Püschel, "Computer Generation of Hardware for Linear Digital Signal Processing Transforms," ACM Trans. Des. Autom. Electron. Syst. **17**(2), 15 (2012).
12. R. Schmogrow, D. Hillerkuss, M. Dreschmann, M. Huebner, M. Winter, J. Meyer, B. Nebendahl, C. Koos, J. Becker, W. Freude, and J. Leuthold, "Real-time software-defined multiformat transmitter generating 64QAM at 28 GBd," IEEE Photon. Technol. Lett. **22**(21), 1601–1603 (2010).
13. UG198 Virtex-5 FPGA RocketIO GTX Transceiver User Guide (2009), Xilinx Inc., Available from: www.xilinx.com.
14. S. Haykin, *Adaptive Filter Theory*, 4th ed. (Prentice Hall USA, 2002).
15. R. Schmogrow, B. Nebendahl, M. Winter, A. Josten, D. Hillerkuss, J. Meyer, M. Dreschmann, M. Huebner, C. Koos, J. Becker, W. Freude, and J. Leuthold, "Error vector magnitude as a performance measure for advanced modulation formats," IEEE Photon. Technol. Lett. **24**(1), 61–63 (2012).

1. Introduction

Orthogonal frequency division multiplexing (OFDM) [1] has attracted much interest within the field of optical communications. Due to its high spectral efficiency and resilience towards fiber dispersion, it has been proposed for a broad range of applications including access and core networks, as well as short links and data centers [1–4]. While first OFDM experiments were based on offline processing, practical applications call for real-time, highly optimized signal processing. Recently, such OFDM transmitters (Tx) [5–7] and receivers (Rx) [8] were demonstrated by employing state-of-the-art field programmable gate arrays (FPGA) along with high speed data converters.

The latest real-time implementations of high speed optical OFDM transmitters include the work published in [6] and [7] where line rates of 101.5 Gb/s and 93.8 Gb/s were reported, respectively. The work presented in [6] used coherent optical OFDM (CO-OFDM) with 16-state quadrature amplitude modulation (16QAM) subcarrier mapping on a single polarization. On the other hand, the results of [7] were achieved with polarization multiplexed CO-OFDM and 4QAM mapping. Both papers considered back-to-back systems without transmission.

This paper describes both the real-time generation and transmission of CO-OFDM signals over 400 km of standard single mode fiber (SSMF) providing more details on a study we previously published in [9]. The real-time transmitter used two FPGAs that encode 85.4 Gb/s of data on 122 subcarriers and a very high speed 128-point inverse fast Fourier transform (IFFT) based on the Spiral Generator [10, 11]. A cyclic prefix (CP) with a length of 25% of the symbol duration is added without the need for additional processing efforts like e. g. multiplexers or first-in first-out buffers (FIFO) enabling dispersion-tolerant transmission over up to 400 km of SSMF. Four pilot tones help to perform frequency offset compensation and carrier phase recovery at the receiver, where data are processed offline. At the receiver, a novel synchronization method is introduced for finding the optimum FFT window position without relying on training symbols. Unlike conventional preamble-based synchronization methods which perform cross-correlations at regular time intervals and let the system run freely in between, the proposed method performs synchronization in a continuous manner ensuring correct symbol alignment at all times.

2. Experimental setup

The experimental setup comprised a real-time software-defined Tx [12] here operated with OFDM, a recirculating fiber loop, and an Agilent N4391A optical modulation analyzer (OMA) as shown in Fig. 1. Two Xilinx Virtex-5 FPGAs (XC5VFX200T) were used to generate the real-time OFDM signal which was then converted into an analog waveform using two 6-bit digital-to-analog converters (DAC) from Micram (operated at 28 GSa/s). The DACs were clocked by an external clock source and used internal programmable clock dividers to provide clocks to the FPGAs. An optical I/Q-modulator encoded the OFDM waveform onto the output of an external cavity laser (ECL) with a center wavelength of 1550 nm and a linewidth of approximately 100 kHz. The resultant signal was amplified using an erbium-doped fiber amplifier (EDFA) and fed to the recirculating loop, which comprised two

#173248 - $15.00 USD Received 24 Jul 2012; revised 27 Aug 2012; accepted 30 Aug 2012; published 5 Sep 2012

amplified spans of 50 km SSMF but no dispersion management. The signal was transmitted along with a holding beam provided by a distributed feedback laser (DFB) for maintaining the EDFA at constant operating point. After a pre-determined number of recirculations, the signal was received by the OMA. The OMA is a coherent receiver comprising two 90° optical hybrids (one for each polarization), balanced photo-detectors and real-time oscilloscopes (80 GSa/s, 32 GHz electrical bandwidth). A second ECL served as local oscillator for the Rx.

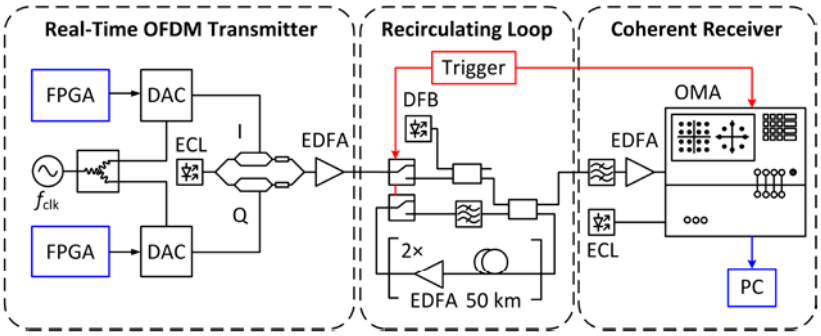

Fig. 1. Experimental setup: an FPGA based real-time Tx with optical I/Q-modulator and external cavity laser (ECL). The amplified signal was sent through a recirculating loop comprising two 50 km spans of SSMF with an EDFA. A DFB laser was used as a holding beam in the loop. A trigger source defined the number of roundtrips by controlling optical switches and the optical modulation analyzer (OMA) used to receive the signal. A second ECL served as a local oscillator. Data were processed on an external PC.

The real-time digital signal processing blocks implemented on the FPGA are shown in Fig. 2. A $2^{15} - 1$ pseudo-random bit sequence generation block (PRBS) generated the data and fed them to a QAM mapper, which mapped each 4 bits into a 16QAM symbol. The PRBS generators on the two FPGAs were synchronized. The IFFT block, which was created using the Spiral Generator framework [11], processed 128 complex inputs to produce the time domain OFDM signal with 10 bits of arithmetic precision. The input to the IFFT included 122 data subcarriers and 4 evenly-spaced pilot tones. The pilot tones were used to perform frequency offset compensation and carrier phase recovery at the receiver. The DC and Nyquist subcarriers (with indices 0 and 64, respectively) were left blank and thus carried no data. The output of the IFFT was clipped to reduce the peak-to-average power ratio (PAPR) of the signal and, hence, reduce the quantization noise in the DAC. This was then followed by a CP insertion stage. The data are passed from the FPGA to the DAC through 24 multi-gigabit transceivers (GTX) operating in parallel which corresponds to four 6-bit samples. The GTXs act as on-chip multiplexers where parallel registers are serialized [13]. The width of these registers was set to 32 bits in previous works, e.g [6]. In this work, the registers were set to be 40 bits wide. In this way, $4 \times 40 = 160$ samples (rather than $4 \times 32 = 128$ samples) were processed within each clock cycle. This corresponds to the 128 point IFFT output plus an additional 32 samples (25%) of cyclic prefix. To enable this operation, the clock divider on the DAC was re-configured to match the new register widths. With this technique, no additional resources on the FPGA needed to be utilized for CP insertion.

The receiver signal processing was carried out offline using Matlab and a block diagram of the main components is shown in Fig. 2. Standard OFDM processing blocks including finite impulse response (FIR) filtering to compensate for the roll-off in the system frequency response, frequency offset compensation, CP removal, FFT, and equalization for channel estimation and dispersion compensation were used. The symbol synchronization however, was achieved using a novel method without relying on a preamble (training symbols). The next section will explain this in more detail.

#173248 - $15.00 USD Received 24 Jul 2012; revised 27 Aug 2012; accepted 30 Aug 2012; published 5 Sep 2012

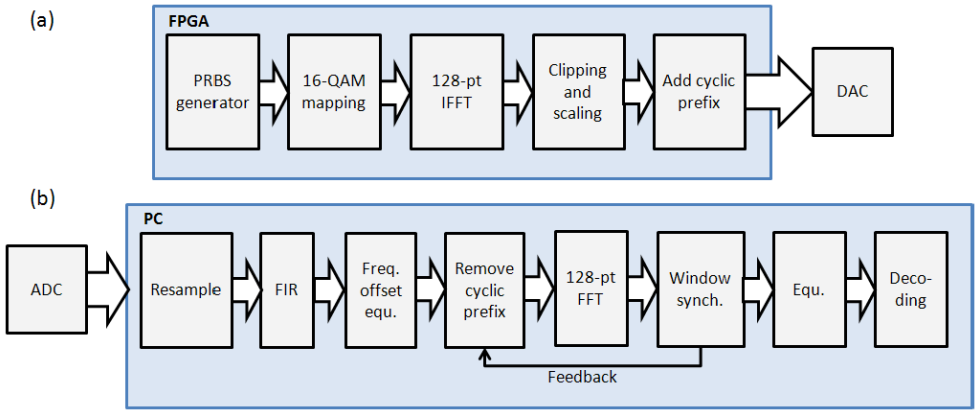

Fig. 2. (a) Real-time FPGA processing blocks of transmitter comprising PRBS generation, 16QAM mapping, an IFFT, clipping and scaling, and cyclic prefix insertion. (b) The receiver offline processing blocks comprise resampling, FIR filtering, frequency offset compensation, cyclic prefix removal, an FFT, window synchronization, equalization (Equ.), and decoding of the data. The signal quality is evaluated through EVM measurements [15].

3. FFT window synchronization

Common synchronization techniques for finding the correct temporal position of the FFT window at the Rx rely mostly on a preamble where training symbols are transmitted regularly and the cross-correlation is performed to determine the correct OFDM symbol position [8]. In this paper, an alternative algorithm is described. It offers enhanced robustness because it performs synchronization as a continuous process along with the reception. In contrast, preamble-based methods let the system run free between synchronization events; therefore, it is prone to errors introduced by drifts in the FFT symbol.

Within one OFDM symbol there are L samples (including CP). Essentially, there are L different starting points for the FFT window, only one of which (after transmission) leads to a correct FFT window position. In order to find the correct position, the received OFDM stream is windowed at different positions ϕ_l where the phase ϕ_l marks the position of the first sample of the window (called a phase because of the periodicity in the FFT window positions). The CP is then removed from each window before an FFT is applied to extract the modulation coefficients C_k as can be seen in Fig. 3(a). In the next step, coefficients C_k obtained from different window positions ϕ_l are vertically arranged and the standard deviations $\sigma(|C_k|)$ are computed, see Fig. 3(b). Finally the standard deviations $\sigma(|C_k|)$ are averaged over several OFDM symbols leading to $\langle\sigma(|C_k|)\rangle_k$ and the minimum of this determines the correct window.

This method is based on the observation that only for a synchronized FFT window the resulting constellation diagram exhibits some regularity (Fig. 3(c) right inset), while otherwise just an unstructured cloud of constellation points is observed (Fig. 3(c) left inset). For back-to-back operation, Fig. 3(c) also shows the resulting averaged $\langle\sigma(|C_k|)\rangle_k$ as a function of the synchronization phase between Tx-IFFT and Rx-FFT window. The optimum phase is found in the region of the flat "trough" which is due to the positioning tolerance introduced by the CP.

As only the modulus of the modulation coefficients is required, no information about the phase of the signals is needed. Hence, the window synchronization is independent of the carrier phase estimation. As we regard the regularity of the non-equalized constellation diagrams, the average power (which may differ for different subcarriers due to e. g. a Tx induced spectral roll-off) does not influence the outcome of the algorithm. Therefore, it can be applied independently of other processing blocks. In a polarization division multiplexing system, the proposed method would be applied after the polarization de-multiplexing stage and is expected to perform equally well.

#173248 - $15.00 USD Received 24 Jul 2012; revised 27 Aug 2012; accepted 30 Aug 2012; published 5 Sep 2012

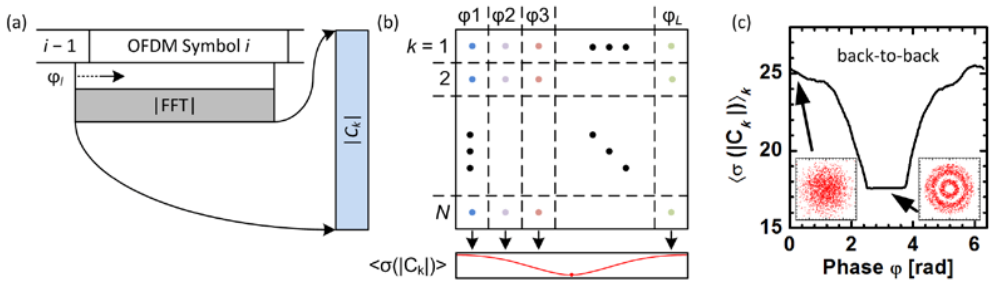

Fig. 3. Schematic design of the FFT window synchronization module and experimental results. (**a**) The OFDM stream is windowed at different starting positions ϕ_l. An FFT extracts the modulation coefficients C_k for each window. (**b**) Coefficients obtained from each window are vertically aligned and the standard deviation $\sigma(|C_k|)$ is computed. The optimum window position is found for the minimum mean value $\langle\sigma(|C_k|)\rangle_k$ of the standard deviation $\sigma(|C_k|)$ of subsequently received random modulation coefficients C_k in subcarrier k, averaged over all subcarriers. (**c**) Output of the window synchronization module in a back-to-back measurement. The flat bottom of the "trough" is due to the phase tolerance introduced by the cyclic prefix.

This technique can be implemented in real-time by performing one FFT per OFDM symbol using an initial windowing position ϕ_l, then calculating $\langle\sigma(|C_k|)\rangle_k$ and using it to determine the next position ϕ_{l+1}. The aim is to minimize $\langle\sigma(|C_k|)\rangle_k$ by changing ϕ_l and the convergence rate can be improved by introducing some intelligence to the search algorithm using the least-mean-squares (LMS) method for example [14]. The optimization variable $\langle\sigma(|C_k|)\rangle_k$ will continue to be calculated for every symbol to detect and correct any drift. To simplify the algorithm for real time implementation, the variance (rather than the standard deviation) could be used, requiring $N + 1$ complex multiplications and $2N$-1 additions if the direct formula is used (N is the number of subcarriers).

4. Transmission experiment and results

The system was tested in the optical back-to-back configuration whereby the recirculating loop (shown in Fig. 1) was bypassed and the output of the transmitter was fed to the receiver directly. The ensemble-averaged 28 GHz spectrum of the OFDM signal is shown in Fig. 4(a). Four pilot tones broadened by the CP can be seen. The roll-off stems from the frequency response of the system and is equalized in the Rx. The signal quality was assessed using error vector magnitude (EVM) [15] and the EVM performance for each subcarrier k is depicted in Fig. 4(b). Most subcarriers had an EVM equal to or better than 10%. Subcarriers close to k = 61 suffered higher EVM than the rest because they are significantly affected by the optical carrier noise which is located close to these subcarriers. Subcarriers close to k = 0 and k = 121 suffer from the system roll-off, as they are located at high frequencies. A clear back-to-back received constellation diagram for subcarrier k = 5 is shown in Fig. 4(c).

Next, the transmission experiment was carried out over several transmission distances and the average EVM over all 122 data subcarriers was measured in each case. Figure 4(d) presents the average EVM as a function of the transmission distance up to 400 km. The figure also indicates the values of EVM corresponding to bit error ratios (BER) of 10^{-3} and 10^{-2}. As can be seen from the figure, the system achieved acceptable EVM for all distances (up to 400 km).

The output of the FFT window synchronization module can be seen in Fig. 5 for both the back-to-back configuration and after 400 km transmission distance. In the back-to-back measurements, suitable windows can be found within the range of the CP of 25% of the symbol length, i. e., within 1 – (1 / 1.25) = 20% (1.26 rad) of the maximum phase difference 2π. This is the trough width in Fig. 5(a). After transmission over 400 km of fiber without dispersion management, the full length of the CP is needed for dispersion compensation. Therefore, only a fixed FFT window position at the minimum $\langle\sigma(|C_k|)\rangle_k$ offers best performance (cf. Fig. 5(b)).

#173248 - $15.00 USD Received 24 Jul 2012; revised 27 Aug 2012; accepted 30 Aug 2012; published 5 Sep 2012

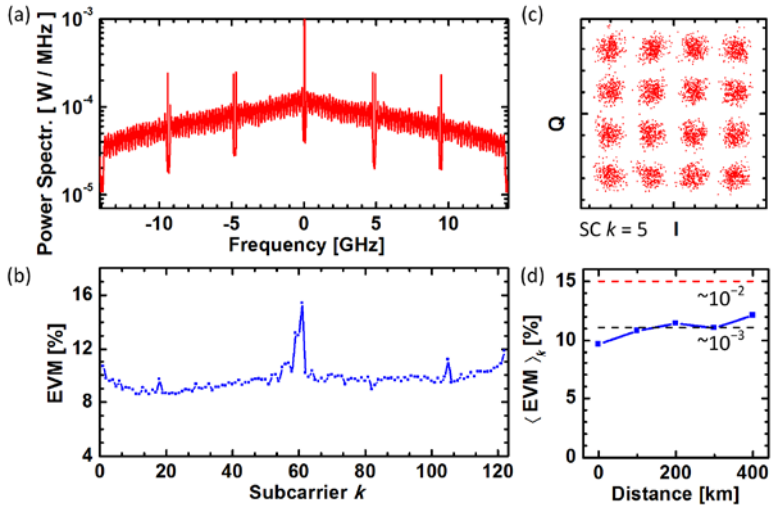

Fig. 4. Experimental results. (a) Measured and ensemble-averaged spectrum. Four pilot tones broadened by the CP are seen. (b) Signal quality, expressed by EVM [15] for different subcarrier positions k in a back-to-back measurement. (c) Constellation diagram of subcarrier k = 5 and back-to-back configuration. (d) Average EVM for all subcarriers after the transmission distance. Values of EVM corresponding to BER of 10^{-3} and 10^{-2} are indicated.

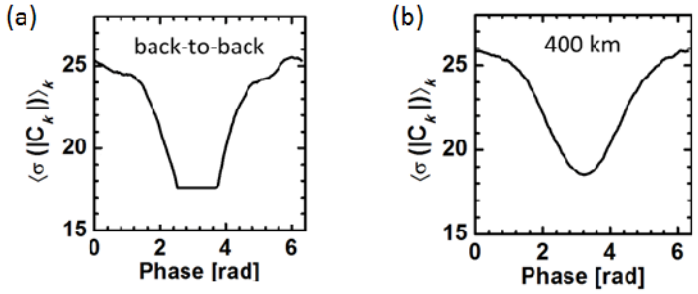

Fig. 5. Output of the synchronization module (a) in the back-to-back configuration and (b) after 400 km transmission.

5. Conclusions

This paper presented the generation and transmission of real-time 16QAM coherent optical OFDM signals. The FPGA-based transmitter ran at 28 GSa/s and achieved a data rate of 85.4 Gb/s. A 25% cyclic prefix was added without the need for additional FPGA processing resources and enabled dispersion-tolerant transmission over up to 400 km of SSMF. A key aspect of the work was the development and demonstration of a novel method for OFDM symbol synchronization without relying on training symbols. Unlike conventional preamble-based synchronization methods which perform cross-correlation at regular time intervals and let the system run freely in between, the proposed method performs synchronization in a continuous manner ensuring correct symbols are used all the time.

Acknowledgments

This work was supported by the projects ACCORDANCE, CONDOR, EuroFOS, Micram Microelectronic GmbH, EPSRC UNLOC (EP/J017582/1), Piano + IMPACT and OTONES, as well as by the Xilinx University Program (XUP), and the Agilent University Relations Program. We further acknowledge financial support from Karlsruhe School of Optics & Photonics (KSOP).

#173248 - $15.00 USD Received 24 Jul 2012; revised 27 Aug 2012; accepted 30 Aug 2012; published 5 Sep 2012